Optimization of the Suspension System of Passenger Cars using the Vibration Model Multi-Objective Method

Tran Thanh An

School of Transportation Engineering, University of Transport Technology, No. 54 Trieu Khuc Street, Thanh Xuan District, Hanoi 100000, Vietnam
antt@utt.edu.vn

Nguyen Van Tuan

School of Transportation Engineering, University of Transport Technology, No. 54 Trieu Khuc Street, Thanh Xuan District, Hanoi 100000, Vietnam
nguyenvantuan@utt.edu.vn (corresponding author)

ABSTRACT

The main functions of the suspension system are the provision of comfort and traction. However, in many cases, paying too much attention to the smoothness of the vehicle has led to incorrect determination of suspension parameters and other problems such as rollover and reduced traction. This study aims to present a design method that optimizes vehicle suspension to improve ride comfort and safety. Based on the structure and specifications of a 29-seat passenger car, this study introduces a general oscillation model of eight degrees of freedom of the passenger car in space. The model allows us to analyze the vibrations of the driver, the body, and the wheels simultaneously under the excitation effect of the road surface and the changes in the vehicle's motion modes. In addition, based on the theory of multi-objective optimization, this study optimized the suspension parameters of the passenger car. The optimized values were: c_d = 100000 N/m, c_{sr} = 154709 N/m, k_{sf} = 7265 Ns/m, c_{sf} = 106193 N/m, k_{sr} = 11297 Ns/m, f_1 = 0.5906 m/s², c_{af} = 6711 Nm/rad, f_2 = 1171 N, c_{ar} = 5683 Nm/rad. The main contribution of the research is the provision of a multi-objective optimization method for the suspension system.

Keywords-multi-objective optimization; suspension; smoothness; protection; model

I. INTRODUCTION

Popular scientific research areas regarding vehicles are the use of biofuels [1, 2], the use of hybrid cars or pure electric cars [3, 4], and the research on vibration [5, 6], which is the subject of this study with the consideration of improving vehicle safety and passenger comfort study. During driving, the driver and passengers are exposed to vibrations from the road surface. Vibrations cause discomfort; reduce working capacity, while their long-term effects can affect health. Authors in [7-9] showed that drivers and passengers in passenger cars are exposed to intense vibrations. Driving comfort depends on human response to vehicle vibration. Vehicle vibration can be caused by various factors such as road roughness, aerodynamic forces, engine vibration, and wheel imbalance [10-12]. Road roughness is considered one of the leading causes of vehicle vibration. It causes the vehicle to suffer from vertical acceleration, making passengers uncomfortable and tired. The suspension is used to reduce vibrations as the connection between the spring assembly and the wheel. The central suspension parameters, including spring stiffness, viscous damping coefficient, and suspension, make up the basic structure of the system [13]. The purpose of every design and shock absorber is to minimize the impact caused by vibrations on other systems or on the occupants of the vehicle. This can be considered as a vibration control system [14-16]. Vibration waves propagate and affect people through the vehicle structure. Changes in a material's structure and composition can affect its ability to propagate vibrational waves and their properties, so all physical relationships must be considered [17-20]. The car suspension system is responsible for suppressing the vibrations of the body and the wheels, ensuring at the same time the smoothness and safety of the car's movement. These are two essential and inseparable goals in the design problem of car suspension systems, especially for passenger cars [21-23]. However, the smoothness and safety of movement are two contradictory indicators. The optimal solution is not a single point but a set of compromise values between two extreme points obtained when optimizing each criterion independently [24-28].

Vibration is an essential dynamic characteristic that determines the smoothness and safety of the car's movement. Under the random effects of the road surface and the change of motion modes, the body will oscillate in the vertical and angular direction around the longitudinal and transverse sway axes of the body [14, 29]. This complex movement has a significant influence on the vibrations of the driver and the vibrations of the wheels.

Computer based numerical analysis is commonly used to design optimal vehicle suspension systems [30]. The advantage of this technique is the reduced cost and time of testing. Rapid scenario-building simulations can be performed with numerical analysis, while, ideally, no physical prototyping is required [31]. Various models, such as the quarter or half-car model, have been used according to random or deterministic road stimulation to provide greater passenger comfort [32, 33]. In [34], a full-car model was used to achieve the best ride comfort by optimizing suspension parameters with design constraints on the vehicle. The genetic algorithm was used in [35] instead of nonlinear programming to enhance driving comfort, resulting to better solutions.

When the car is in motion many factors may cause oscillations. Safety and smooth motion are two critical dynamic parameters, inseparable but contradictory to each other during movement, which are mainly determined by the quality of the suspension system. In this study, based on the structure and specifications of the 29-seat passenger car, the main objective is to introduce a general oscillation model of eight degrees of freedom of the passenger car in space, allowing to analyze simultaneously the vibration of the driver, the body, and the wheels under the stimulus effect of the road surface and the change of the vehicle's motion modes. Additionally, based on the theory of multi-objective optimization, the parameters of the passenger car's suspension system were optimized in order to meet the two criteria of safety and smoothness at the same time.

II. METHODOLOGY

A. Experimental Setup

In the study of automobile vibration, it is necessary to conduct empirical research to take data as input parameters to obtain a model with high accuracy and reliability. A pilot study on a 29-seat passenger car was conducted to get data to run the car vibration model. The experimental results are also the basis for standardizing the theoretical model for studying the essential dynamical characteristics of cars under different moving conditions. The first part of the data used to run the model will take the following parameters:

- The mass of the cars selected for survey.

- Stiffness of suspension, tires, and driver's seat.

- Damping coefficient of the suspension system and driver's seat.

- Acceleration oscillations at various positions on the vehicle.

The data results are shown in Table I.

The second part was used to validate the model: The experiment was conducted by measuring the oscillation acceleration at several locations on the car, as illustrated in Figure 1, where position (1) is on the front live axle, left; position (2) on the rear live axle, left; position (3): on the vehicle body, on the left, in the vertical plane perpendicular to the longitudinal axis of the vehicle and passing through the center of gravity of the vehicle; position (4) on the body of the car, on the left, corresponding to the rear live axle; position (5) on the vehicle body, on the right, in the vertical plane perpendicular to the longitudinal axis of the vehicle and passing through the center of gravity of the vehicle; and position (6) is on the driver's seat.

The experiment used an LMS Scadas Mobile oscilloscope (SCM05), 16-channel type, with an accompanying software package manufactured in Belgium (Figure 2). This device has the following basic characteristics: Designed according to MIL-STD-810F military standards, capable of withstanding harsh operating conditions and shock, high mobility, can use 110/220V AC or 9V to 36V DC power source, cooling using circulating evaporation tube technology without using fans (can cause interference), independent 102.4 kHz maximum sampling rate on all channels (not shared or interdependent), 24-bit signal resolution, Signal/noise ratio of 105 dB, maximum total data collection speed is 2.2 million samples/s, while it supports various types of sensors (acceleration, temperature, strain, pressure, etc.).
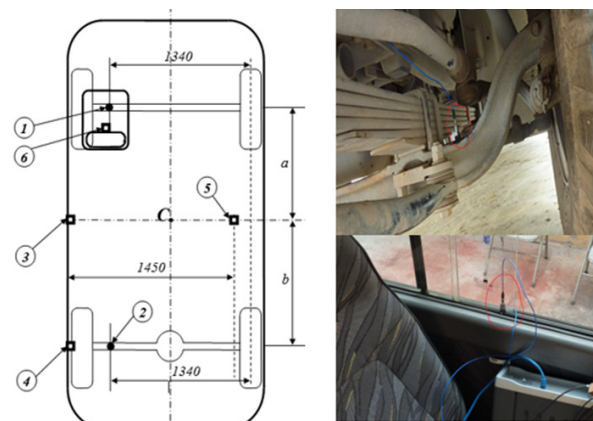

Fig. 1.   Diagram of accelerometer mounting locations. ● Location on the live axle, ▢ location on the body of the vehicle.
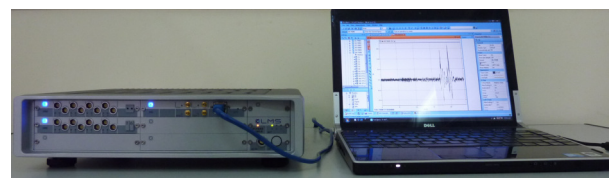

Fig. 2.   Data collector with the laptop running the software.

B. Characteristics of the Studied Car

The 29-seat vehicle is being used to transport passengers. Vehicles with suspension systems of 29-seat passenger cars are dependent types. This suspension system has a design of

wheels connected by a single bridge girder, which will touch the vehicle's body. Therefore, the oscillations of the wheels will affect and depend on each other. The suspension system on the car has a semi-elliptic leaf spring type elastic element consisting of 5 leaf springs at the front and 7 leaves at the rear. The suspension system has reinforced, hydraulic shock tubular absorbers, with a horizontal stabilizer bar. The vehicle specifications are shown in Table II.

TABLE I.   EXPERIMENTAL RESULTS OF THE CAR VIBRATION MODEL

Specification	Value
Total weight, m_{car} (kg)	6087
Distribution of the front live axle, m_f (kg)	2506
Distribution of rear live axle, m_r (kg)	3581
Weight of the part to be hung, m_s (kg)	5394
Distribution of the front live axle (kg)	2240
Distribution of front live axle (kg)	3154
The mass of the part that is not hanging on the front live axle, m_{uf} (kg)	266
The mass of the part that is not sprung on the rear live axle, m_{ur} (kg)	427
Weight of driver and driver's seat, m_d (kg)	75
Mass moment of inertia sprung about the axis O_x, J_y (kgm²)	19632
Stiffness of the front suspension, c_{sf} (N/m)	177007
Stiffness of the rear suspension, c_{sr} (N/m)	193844
Front suspension damping factor, k_{sf} (Ns/m)	7733
Rear suspension damping factor, k_{sr} (Ns/m)	9804
Torsion stiffness of the front differential bar, c_{af} (Nm/rad)	5000
Torsion stiffness of rear differential bar, c_{ar} (Nm/rad)	5000
Stiffness of the front tire, c_{uf} (N/m)	493211
Rear tire stiffness, c_{ur} (N/m)	986422
Vehicle wheelbase, L (m)	4.085
Distance from center of gravity to front differential, l_f (m)	2.400
Distance from center of gravity to following differential, l_r (m)	1.685
Driver's seat stiffness, c_d (N/m)	52537
Driver's seat resistance coefficient, k_d (Ns/m)	1000

TABLE II.   SPECIFICATIONS OF THE 29-SEAT PASSENGER CAR

Specification	Value
Range of vehicle	29-seat bus
Dimensions: Length × Width × Height (mm)	7060×2080×2750
Self-weight (kg)	4200
Number of people allowed to return including the driver	29
Carry-on luggage (kg)	305
Total mass of the car (kg)	6100
Maximum speed of the vehicle (km/h)	95
Maximum slope that the vehicle can overcome (%)	42.95
Acceleration time of the vehicle from the time of departure to the end of the distance of 200 m (s)	19
Oscillation frequency of the part to be suspended (times/min)	118.2/94.6
Vehicle braking distance at 30 km/h at idle/full load (m)	7.23/7.82
Braking acceleration of the vehicle at 30 km/h at no load/full load (m/s²)	6.86/6.34
Minimum turning radius of the vehicle according to the outboard front wheel track (m)	7.4
Code of front and rear tires	7.00R16
Number of tweezers in the front suspension system	5
Number of tweezers in the rear suspension system	7

C. Theoretical Basis of the Passenger Car Space Oscillation Model

With the above assumptions, the vibration model of the passenger car in space, taking into account the driver's vibration, can be built as described in Figure 3. In the model,

the driver and the seat are considered as a point of mass m_d linked to the body by an elastic element with stiffness c_d and a damping element with a damping coefficient k_d.
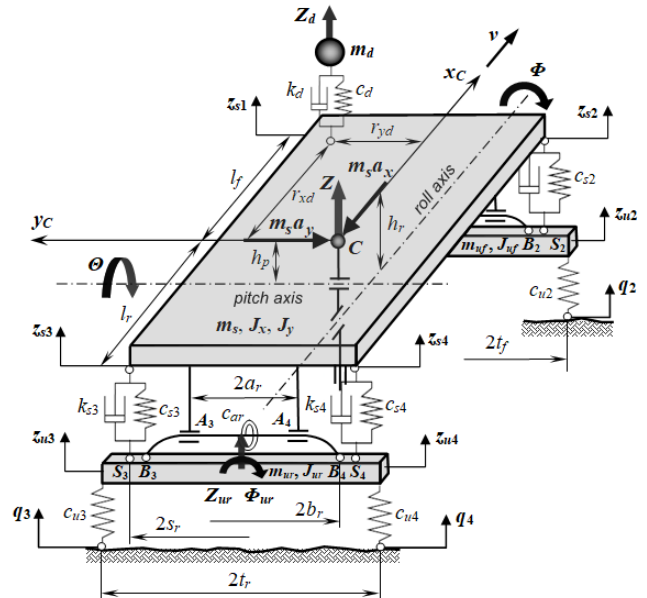

Fig. 3.   Vibration model of the passenger car in space.

The vehicle body has mass m_s and moments of inertia J_x and J_y. The inertia characteristics of the front and rear axles are the mass m_{uf}, m_{ur} and the moments of inertia of the mass J_{uf} and J_{ur}. The dependent suspension system has a drag coefficient k_{si} and stiffness c_{si} that links the axles to the body. The action of the front and rear stabilizer bars is characterized by torsional stiffness c_{af} and c_{ar}. The differential connection and the road surface are done through wheels with c_{ui} stiffness. The wheels are always in contact with the road surface with the corresponding bumpy amplitude q_i (i = 1,2,3,4). The model has 8 degrees of freedom, including:

- Vertical displacement of the driver Z_d;

- The three movements of the vehicle body are the vertical displacement of the center of gravity Z, the longitudinal swing angle Θ around the pitch axis in a distance h_p from the center of gravity, and the angle of roll Φ about the roll axis in a distance h_r from the center of gravity. Vectors of generalized coordinates of the vehicle body describe these three movements:

$$y_s = [Z, \Phi, \Theta]^T \qquad (1)$$

- The four degrees of freedom of the unsuspended mass are the vertical displacement Z_{uf}, Z_{ur} and the angular displacement Φ_{uf}, Φ_{ur} of the front and rear axles which are represented by vectors of the generalized coordinates of the unsuspended mass:

$$y_u = [Z_{uf}, Z_{ur}, \Phi_{uf}, \Phi_{ur}]^T \qquad (2)$$

The eight degrees of freedom of the model can be represented by vectors of the model's generalized coordinates:

$z = [Z_d, Z, \Phi, \Theta, Z_{uf}, Z_{uf}, \Phi_{uf}, \Phi_{ur}]^T = [Z_d, y_s^T, y_u^T]^T$ (3)

The external forces acting on the model are the excitations from the pavement q_i at the four wheels and the inertial forces located at the center of gravity: $F_{jx} = m_s.a_x$ in the longitudinal direction and $F_{jy} = m_s a_y$ in the horizontal direction.

Based on the D'alembert principle [36], separating the connection between the car body, the driver's seat, and the bridges, considering the balance of the bodies after adding the inertial and bonding force components, we can get a system of oscillation equations corresponding to 8 degrees of freedom of the model as follows:

The first equation represents the driver's oscillation; the following three equations describe the body's vibrations (the mass is suspended), and the last four represent the oscillations of the front and rear axles (the mass is not broken).

where:

- F_d represents the bonding force between the driver's seat and the body, F_{si} and F_{ui} represent the bonding force of the suspension system at the ith wheel position and the bonding force between the with wheels and the road surface (i = 1,2,3,4);

- M_{af} and M_{ar} represent the anti-roll moment generated by the lateral stabilization system at the front and rear axles.

- r_s and r_u are the coordinates of the measuring points (r_{sxi}, r_{syi}, r_{uxi}, r_{uyi}) as follows:

  o The first point on the left front wheel has coordinates: (l_f, s_f, l_f, t_f).

  o The second point on the front wheel has coordinates: (l_f, -s_f, l_f, -t_f).

  o The third point on the left rear wheel has coordinates: (-l_r, s_r, -l_r, t_r).

  o The fourth point on the rear wheel must have the coordinates: (-l_r, -s_r, -l_r, -t_r).

$$\begin{cases} m_d \ddot{Z}_d = -F_d \\ m_s \ddot{Z} = -\sum_{i=1}^{4} F_{si} + F_d \\ (J_x + m_s h_r^2)\ddot{\Phi} = -\sum_{i=1}^{4} F_{si} r_{syi} + M_{af} + M_{ar} + F_d r_{yd} + m_s a_y h_r \\ (J_y + m_s h_p^2)\ddot{\Theta} = -\sum_{i=1}^{4} F_{si} r_{sxi} - F_d r_{xd} - m_s a_x h_p \\ m_{uf} \ddot{Z}_{uf} = \sum_{i=1}^{2}(F_{si} - F_{ui}) \\ m_{ur} \ddot{Z}_{ur} = \sum_{i=3}^{4}(F_{si} - F_{ui}) \\ J_{uf} \ddot{\Phi} = -\sum_{i=1}^{2} F_{si} r_{syi} - \sum_{i=1}^{2} F_{ui} r_{uyi} + M_{af} \\ J_{ur} \ddot{\Theta} = -\sum_{i=3}^{4} F_{si} r_{syi} - \sum_{i=3}^{4} F_{ui} r_{uyi} + M_{ar} \end{cases}$$ (4)

D. Simulation Model of the Passenger Car in Space

Based on the mathematical model and the system of state space equations, it is possible to establish a Matlab - Simulink model to solve the system of equations of oscillation of the passenger car in space, as shown in Figure 4. In the Figure, there are input parameter blocks "inputs" describing the vector of generalized external forces or the excitation vectors (moment of inertia around the longitudinal and lateral shaking axis, and the excitation of the road surface at wheel positions); model block "model" represents the system of equations for passenger car vibration in state space form; The block of output parameters "outputs" defines the vector of the output parameters or evaluation parameters of the model y (driver's oscillation acceleration $\ddot{Z}_d$, vehicle body oscillation acceleration $\ddot{Z}, \ddot{\Phi}, \ddot{\Theta}$, dynamic load at the wheels, relative displacement of suspended and unsustained masses at wheel positions $\Delta_{zi} = z_{si} - z_{ui}$).
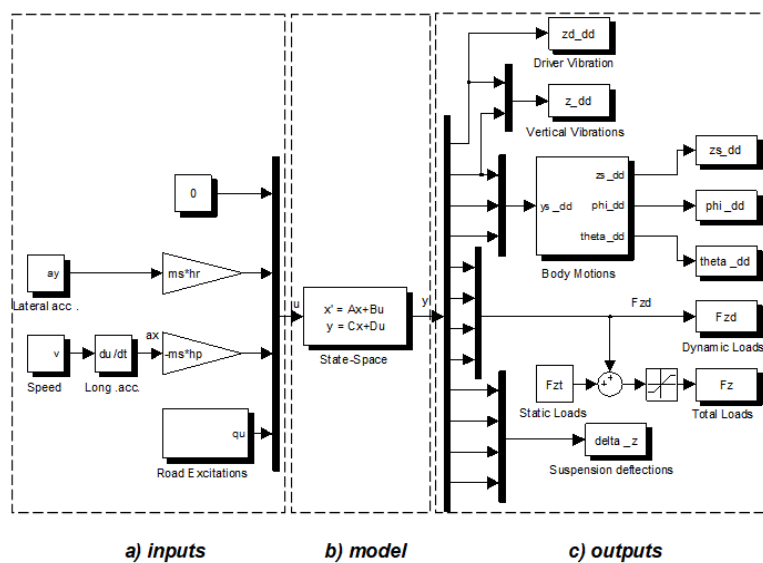

Fig. 4.   The 8-degree of freedom vibration model of the passenger car in Matlab – Simulink.

E. Multi-Objective Optimization Application with Follow-up System

We can use the intercept method for a problem with only two objectives. This is also a commonly used method in the field of automotive optimization. The specific content of the blocking function method [37] can be seen in Figure 5.
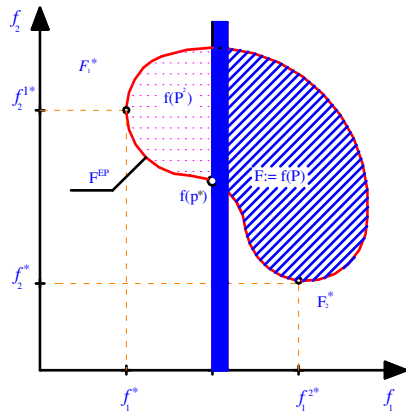

Fig. 5. Block function method for the two-objective optimization problem.

It shows that the essence of the intercept method is to choose an objective $f_h(p)$ to optimize while the remaining objectives are put into the form of bound inequality:

$$\min_{p \in P^r} f_h(p) \quad with \quad P^r := \left\{ p \in P \big| f_i(p) \le \varepsilon_i, i \in I_n / \{r\} \right\} \quad (5)$$

For a two-objective optimization problem, the intercept method can be expressed as follows:

$$\min_{p \in P^2} f_2(p) \quad with \quad P^2 := \left\{ p \in P \big| f_1(p) \le \varepsilon_1 \right\} \quad (6)$$

In the above formula, ε_1 represents an upper bound for the objective function f_1 and can be viewed as a scalar parameter. By varying the constraints ε_1, it is possible to obtain different optimal points on the Pareto boundary.

From Figure 5, we can imagine the working process of the intercept method for the two-objective optimization case. With f_2 is the objective to be optimized while f_1 is considered as a constraint to $f_1 \le \varepsilon_1$, the multi-objective optimization problem is reduced to a single-objective optimization; by minimizing an individual objective function f_2 and adding a constraint condition $f_1 \le \varepsilon_1$. With this constraint, the original objective space can be reduced to $F_2 = f(P^2)$, which is the upper and left part of the space F and is limited by ε_1. The solution to the problem depends heavily on the value of constraint ε_1.

Suppose $\varepsilon_1 < f_1^* := f_1(P_1^*)$ is chosen; when the value of ε_1 changes, there will be no possible solutions to the given problem. On the other hand, if $\varepsilon_1 > f_1^{2*} := f_1(P_2^*)$ is selected, the entire survey space is feasible, and the problem is to find a solution F_2^* as a result. Scores F_1^* and F_2^* are the independent optimal points of each objective function f_1 and f_2. When only the objective function f_2 is minimal, its smallest value is f_2^*; corresponding to this value, we will determine a point P_2^* in the parameter domain.

F. Model Validation

For quantitative evaluation, it is necessary to calculate the relative error. The relative error is the ratio of the square error to the practical value of the quantity calculated from theory according to the following mathematical expression [38]:

$$\sigma = \frac{\delta}{X_{ET}} \quad (7)$$

where σ is the relative error between theory and experiment, δ is the square difference between theoretical simulation results and experimental results, X_{ET} is the effective value calculated from theory. The calculation results from the theoretical and the experimental values give us the following relative error values:

$$\begin{aligned} \sigma_{\ddot{Z}} &= 7.32 \ (\%) \\ \sigma_{\ddot{Z}_d} &= 5.47 \ (\%) \\ \sigma_{\ddot{\Phi}} &= 6.25 \ (\%) \\ \sigma_{\ddot{\Theta}} &= 4.16 \ (\%) \end{aligned} \quad (8)$$

III. RESULTS AND DISCUSSION

A. Model Validation

The calculation results of the relative error (8) between the value obtained from the theory corresponding to the model shown in Figure 6 were normalized, and the value obtained from the experiment validates the reliability of the theoretical model. On that basis, a theoretical model can be used to analyze the essential dynamical characteristics of passenger cars in different moving conditions and is a scientific basis for designing an optimal suspension system.

B. Optimal Results using the Suspension Parameters and the Intercept Method

There are many methods to solve the multi-objective optimization problem. In this study, the intercept method (ε - Constraint Method) is used to solve the problem of optimizing the smoothness and safety of passenger cars. The method aims to reshape the two-objective optimization problem to a one-objective optimization problem of the motion safety criterion f_2; while the smoothness criterion f_1 is expressed as a constraint inequality limited by the intercept function ε:

$$\min_{p \in P^2} f_2(p), P^2 := \left\{ p \in P \big| f_1(p) \le \varepsilon_1 \right\} \quad (9)$$

To solve the problem, it is first necessary to determine the individual minima F_1^* and F_2^* thanks to the optimization problems of separate objectives in (10) and (11):

$$\min_{p \in P} f_1(p) = \frac{1}{2} \left(\sqrt{\frac{1}{T} \int_0^T \ddot{Z}_d^2 dt} + \sqrt{\frac{1}{T} \int_0^T \ddot{Z}^2 dt} \right)$$

$$P := \begin{cases} p = \left[c_d, k_{sf}, k_{sr}, c_{sf}, c_{af}, c_{ar} \right]_{(7 \times 1)}^T \big| p^l \le p \le p^u \\ p^l = \left[25000, 5000, 5000, 100000, 100000, 0, 0 \right]^T \\ \max\left(\max |z_s - z_u| \right) \le 0.05 \\ m_{sf} \, g \, / \, 2 c_{sf} \le 0.10 \\ m_{sr} \, g \, / \, 2 c_{sr} \le 0.10 \end{cases} \quad (10)$$

$$\min_{p \in P} f_2(p) = \frac{1}{4}\left(\sum_{i=1}^{4}\sqrt{\frac{1}{T}\int_0^T F_{zdi}^2 dt}\right)$$

$$P := \begin{cases} p = \left[c_d, k_{sf}, k_{sr}, c_{sf}, c_{af}, c_{ar}\right]_{(7x1)}^T \big| p^l \leq p \leq p^u \\ p^l = \left[25000, 5000, 5000, 100000, 100000, 0, 0\right]^T \\ \max\left(\max|z_s - z_u|\right) \leq 0.05 \\ m_{sf} g / 2c_{sf} \leq 0.10 \\ m_{sr} g / 2c_{sr} \leq 0.10 \end{cases} \quad (11)$$

After solving the above problems with the initial value (starting point) $p^0 = p^l$, it is possible to determine the positions of the individual minima in the target domain thanks to the vectors:

$$f_1^* = \left[f_{1min}, f_{2max}\right]^T = \left[0.5755, 1206\right]^T \quad (12)$$
$$f_2^* = \left[f_{1max}, f_{2min}\right]^T = \left[0.6058, 1144\right]^T$$

The value domain f_1 is divided into $N = 19$ points equidistant between the two endpoints f_{1min} and f_{1max}. The distance between the points is determined by:

$$\Delta\varepsilon_1 := \frac{f_1^{2*} - f_1^*}{N+1} = \frac{f_{1max} - f_{1min}}{N+1} \quad (13)$$
$$= \frac{0.6058 - 0.5755}{19+1} = 0.001515$$

The Edworth-Pareto (EP) optimal solution set in the target domain shown in Figure 7 is the result obtained after solving N simple optimization problems (13) corresponding to the intercept function value ε_{1k} varying from f_{1max} to f_{1min}.

$$\varepsilon_{1k} = f_{1max} - k\Delta\varepsilon_1 \quad (14)$$

Specific values of the problem of optimizing the suspension system of 29-seat passenger cars are given in Figure 8, where $k_{sf} = k_{s1} = k_{s2}$, $k_{sr} = k_{s3} = k_{s4}$, $c_{sf} = c_{s1} = c_{s2}$, $c_{sr} = c_{s3} = c_{s4}$.

It should be noted that all the points in Figure 7 with corresponding values given in Figure 8 are optimal EP solutions. Depending on the operating conditions of the passenger car, we can choose the optimal solution circled, as shown in Figure 6, as the final result of the problem of optimizing the 29-seat passenger car suspension system. From there, it is possible to determine the optimal values of the design parameter p^* and the objective function f^* corresponding to the selected solution as follows:

$$p^* = \left[100000, 7265, 11297, 106193, 154709, 6711, 5683\right]^T$$

$$p = \left[52537, 7733, 9804, 177007, 193844, 5000, 5000\right]^T \quad (15)$$

Compared to the original car:

$$f = \left[1.032, 1245\right]^T \quad (16)$$

The smoothness and safety of passenger cars after optimizing the suspension system are improved.
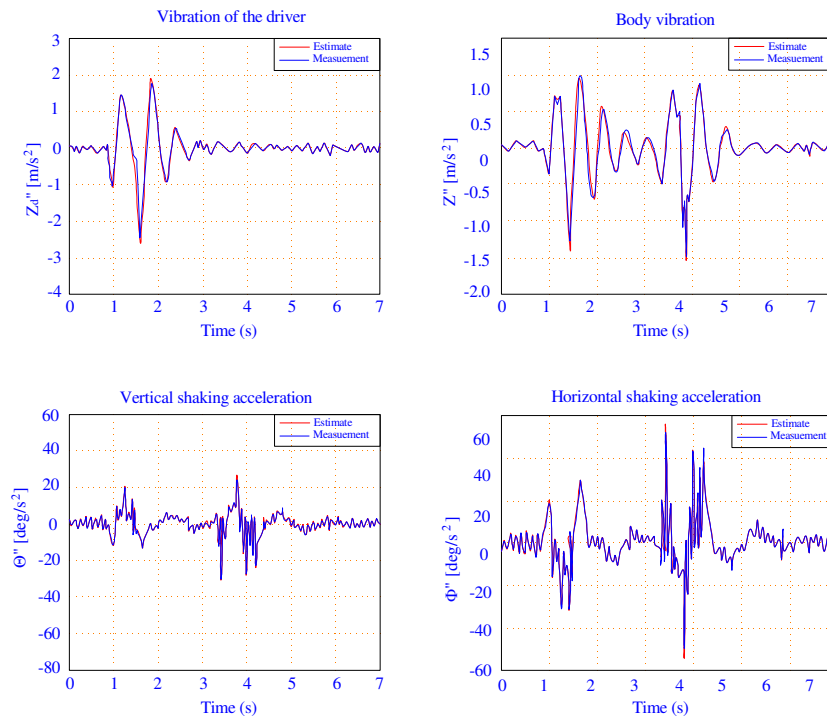

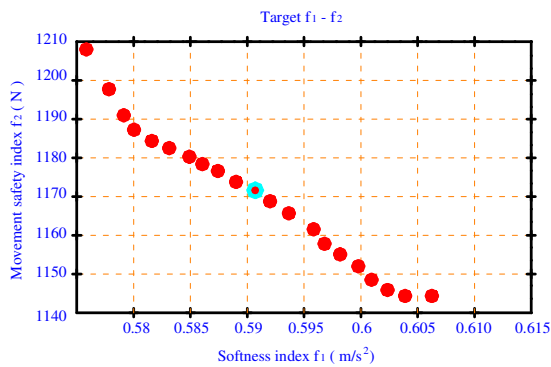Fig. 6.   Vibration acceleration of driver and body, v = 13 km/h.

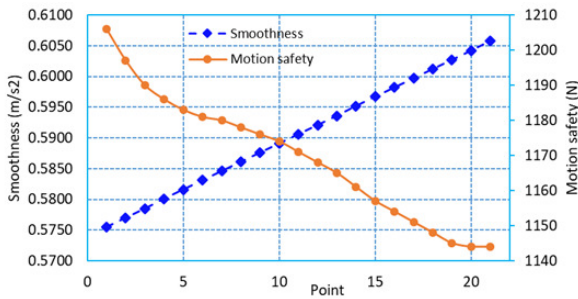Fig. 7.　　The optimal solution set in the target space domain.

Fig. 8.　　Optimal results of the 29-seat passenger car suspension system.

C. Evaluation of the Vibrations of the Passenger Car with Optimal Suspension in the Time Domain

In Figure 9, the random excitation amplitudes of the pavement corresponding to the left wheels (dark color) and the right wheels (light color) are simulated according to the ISO standard with average road quality. The simulation results of the vibration acceleration of the driver, the body vibration acceleration, and the load on the wheels in the case of moving speed v = 5 km/h are illustrated in Figure 10 and 11, respectively.

Based on the simulation model of passenger cars in space (Figure 4) and the results of the optimization problem with different modes of movement speed, it can be seen that the indicators of smoothness f_1 and safety of motion f_2 are significantly improved (Table III).
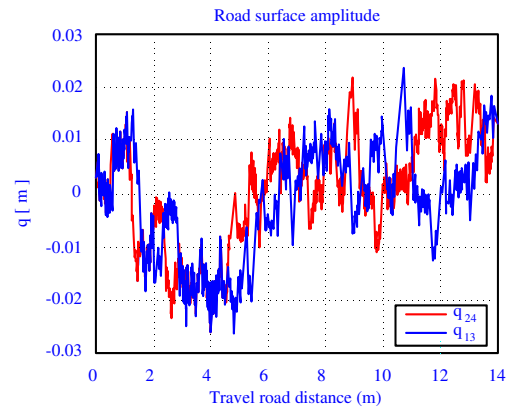

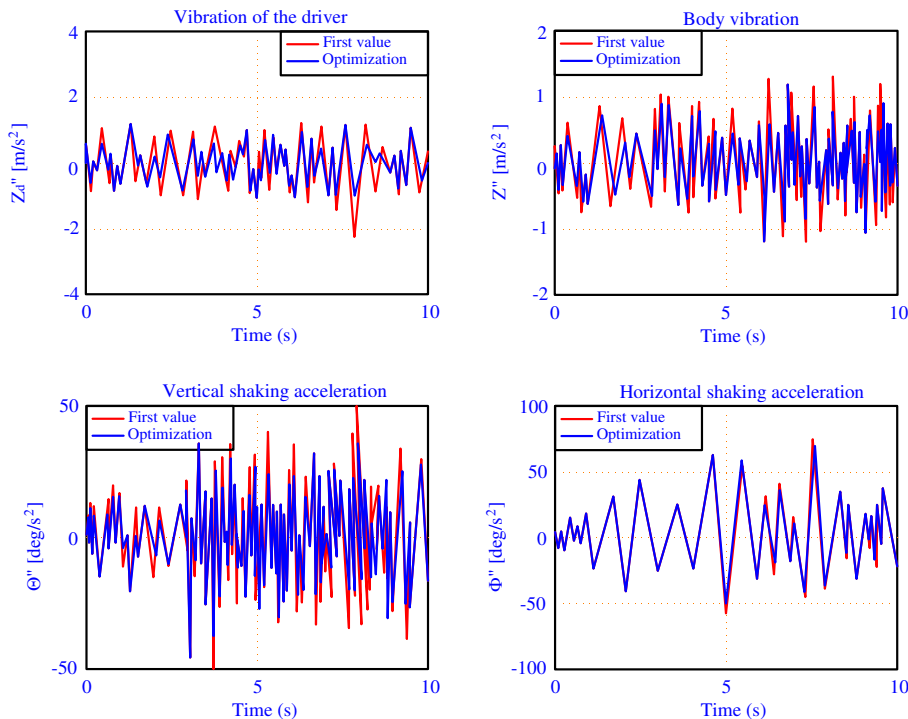Fig. 9.　　Random excitation amplitude of the pavement.

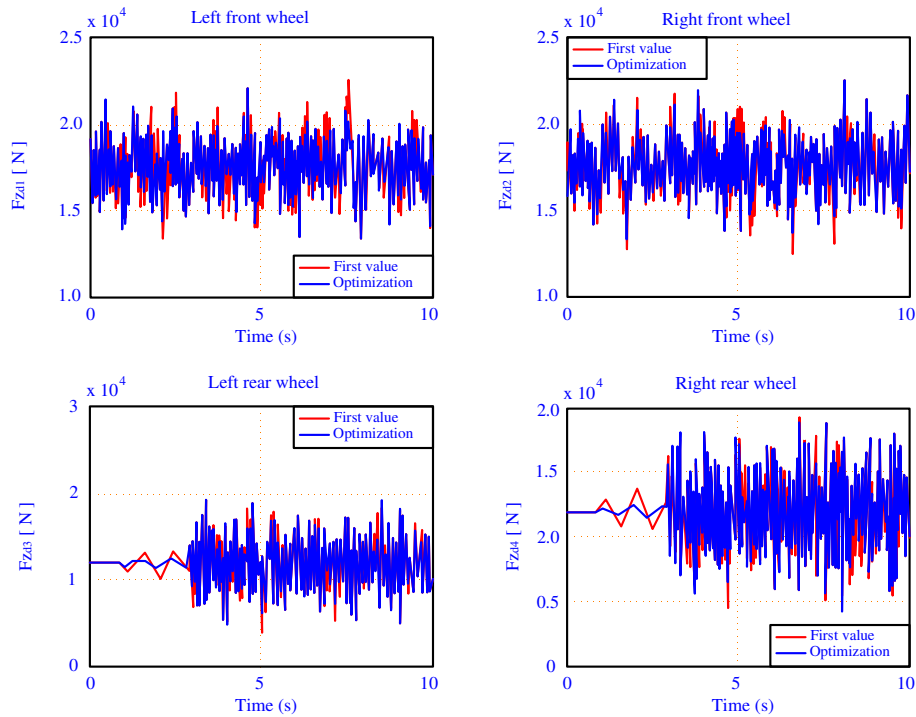Fig. 10.　　Vibration acceleration of driver and body, v = 5 km/h.

Fig. 11.   Variation of wheel load, v = 5 km/h.

TABLE III.   VEHICLE VIBRATION EVALUATION CRITERIA BEFORE AND AFTER OPTIMIZATION

Suspension system	Softness index f_1 [m/s^2]	Movement safety index f_2 [N]
5 km/h		
Original suspension	0.6858	1738.4
Optimal suspension system	0.5120	1337.7
Original suspension	-25.34%	-23.06%
10 km/h		
Original suspension	0.9540	2578.2
Optimal suspension system	0.7121	2065.9
Rate of change	-25.36%	-19.87%
20 km/h		
Original suspension	1.3188	3902.3
Optimal suspension system	0.9911	3306.4
Original suspension	-24.85%	-15.26%
40 km/h		
Original suspension	1.6436	5063.3
Optimal suspension system	1.2199	4492.2
Original suspension	-25.78%	-11.27%
80 km/h		
Original suspension	1.8605	6527.9
Optimal suspension system	1.3931	5854.9
Original suspension	-25.12%	-10.30%

IV.   CONCLUSION

It is possible to use theoretical models to study the fundamental dynamics of cars in different moving conditions. It is also the scientific basis for the optimal design of the suspension system of passenger cars in particular and automobiles in general. Safety and smoothness are the main goals when designing an automotive suspension system. In this study, based on the 8-degree-of-freedom spatial oscillation model of passenger cars, and taking into account the vibrations of the driver, a multi-objective optimization application method to determine the parameters of the optimal suspension system and the smoothness and safety of car movement is introduced.

After conducting experiments as the basis for standardizing the parameters of the theoretical model, the results of calculating the relative error between the value obtained from the theory and the experiment ($\sigma_{\ddot{Z}}$ = 7.32%; $\sigma_{\ddot{Z}_d}$ = 5.47%; $\sigma_{\ddot{\Phi}}$ = 6.25%; $\sigma_{\ddot{\Theta}}$ = 4.16%) showed the reliability of the theoretical model.

Based on the 8-degree-of-freedom spatial oscillation model of passenger cars, and taking into account the vibrations of the driver, the chosen method to solve the optimal problem simultaneously with two objective functions of safety and smoothness determined the optimal parameters of the suspension system: c_d = 100000 N/m, c_{sr} = 154709 N/m, k_{sf} = 7265 Ns/m, c_{sf} = 106193 N/m, k_{sr} = 11297 Ns/m, f_1 = 0.5906 m/s^2, c_{af} = 6711 Nm/rad, f_2 = 1171 N, c_{ar} = 5683 Nm/rad.

The results of the oscillation of 29-seat passenger cars in the time domain correspond to different motion modes and the frequency domain. The results showed that the vehicle's smoothness and safety indicators were significantly improved compared to the original suspension system;

REFERENCES

[1]   W. Zhao, Z. Li, G. Huang, Y. Zhang, Y. Qian, and X. Lu, "Experimental investigation of direct injection dual fuel of *n*-butanol and biodiesel on Intelligent Charge Compression Ignition (ICCI) Combustion mode," *Applied Energy*, vol. 266, May 2020, Art. no. 114884, https://doi.org/10.1016/j.apenergy.2020.114884.

[2] N. P. Truong, N. X. Khoa, and N. Van Tuan, "Building a research model for the combustion process of fuel in a constant volume combustion chamber," *International Journal of Sustainable Engineering*, vol. 17, no. 1, pp. 1–15, Dec. 2024, https://doi.org/10.1080/19397038.2024.2329178.

[3] D. Mohanraj, J. Gopalakrishnan, B. Chokkalingam, and L. Mihet-Popa, "Critical Aspects of Electric Motor Drive Controllers and Mitigation of Torque Ripple—Review," *IEEE Access*, vol. 10, pp. 73635–73674, Jan. 2022, https://doi.org/10.1109/ACCESS.2022.3187515.

[4] T. T. An, D. Q. Minh, and N. V. Tuan, "Calculation And Design Of Power Split Device On A Hybrid Vehicle," *Journal of Applied Science and Engineering*, vol. 27, no. 6, pp. 2643–2651, Jun. 2024, https://doi.org/10.6180/jase.202406_27(6).0005.

[5] J. P. Pauwelussen, *Essentials of Vehicle Dynamics*. Waltham, MA, USA: Butterworth-Heinemann, 2014.

[6] J. Balkwill, *Performance Vehicle Dynamics: Engineering and Applications*. Waltham, MA, USA: Butterworth-Heinemann, 2017.

[7] C. Wang, X. Zhao, R. Fu, and Z. Li, "Research on the Comfort of Vehicle Passengers Considering the Vehicle Motion State and Passenger Physiological Characteristics: Improving the Passenger Comfort of Autonomous Vehicles," *International Journal of Environmental Research and Public Health*, vol. 17, no. 18, Jan. 2020, Art. no. 6821, https://doi.org/10.3390/ijerph17186821.

[8] O. O. Okunribido, S. J. Shimbles, M. Magnusson, and M. Pope, "City bus driving and low back pain: A study of the exposures to posture demands, manual materials handling and whole-body vibration," *Applied Ergonomics*, vol. 38, no. 1, pp. 29–38, Jan. 2007, https://doi.org/10.1016/j.apergo.2006.01.006.

[9] G. Litak, M. Borowiec, J. Hunicz, G. Koszalka, and A. Niewczas, "Vibrations of a delivery car excited by railway track crossing," *Chaos, Solitons & Fractals*, vol. 42, no. 1, pp. 270–276, Oct. 2009, https://doi.org/10.1016/j.chaos.2008.11.020.

[10] D. Khan and R. Burdzik, "Measurement and analysis of transport noise and vibration: A review of techniques, case studies, and future directions," *Measurement*, vol. 220, Oct. 2023, Art. no. 113354, https://doi.org/10.1016/j.measurement.2023.113354.

[11] R. Burdzik and L. Konieczny, "Application of Vibroacoustic Methods for Monitoring and Control of Comfort and Safety of Passenger Cars," *Solid State Phenomena*, vol. 210, pp. 20–25, 2014, https://doi.org/10.4028/www.scientific.net/SSP.210.20.

[12] R. Burdzik and L. Konieczny, "Research on structure, propagation and exposure to general vibration in passenger car for different damping parameters," *Journal of Vibroengineering*, vol. 15, no. 4, pp. 1680–1688, Dec. 2013.

[13] Z. Lu, S. Li, S. Felix, J. Zhou, and B. Cheng, "Driving comfort evaluation of passenger vehicles with natural language processing and improved AHP," *Journal of Tsinghua University*, vol. 56, no. 2, pp. 137–143, Feb. 2016, https://doi.org/10.16511/j.cnki.qhdxxb.2016.22.004.

[14] J. Tuma, J. Simek, J. Skuta, and J. Los, "Active vibrations control of journal bearings with the use of piezoactuators," *Mechanical Systems and Signal Processing*, vol. 36, no. 2, pp. 618–629, Apr. 2013, https://doi.org/10.1016/j.ymssp.2012.11.010.

[15] R. Xu and U. Ozguner, "Sliding mode control of a class of underactuated systems," *Automatica*, vol. 44, no. 1, pp. 233–241, Jan. 2008, https://doi.org/10.1016/j.automatica.2007.05.014.

[16] F. Pehlivan, I. Esen, and C. Mizrak, "Vibration analysis of half rail vehicle model with 10 degrees of freedom based on mechanical-electrical analogy theory," *International Journal of Heavy Vehicle Systems*, vol. 28, no. 4, pp. 521–541, Jan. 2021, https://doi.org/10.1504/IJHVS.2021.118245.

[17] P. Folega and G. Siwiec, "Numerical analysis of selected materials for flexsplines," *Archives of Metallurgy and Materials*, vol. 57, no. 1, pp. 185–191, 2012, https://doi.org/10.2478/v10172-012-0008-5.

[18] F. Pehlivan, C. Mizrak, and I. Esen, "Modeling and Validation of 2-DOF Rail Vehicle Model Based on Electro–Mechanical Analogy Theory Using Theoretical and Experimental Methods," *Engineering, Technology & Applied Science Research*, vol. 8, no. 6, pp. 3603–3608, Dec. 2018, https://doi.org/10.48084/etasr.2420.

[19] J. Mencik, "Determination of parameters of visco-elastic materials by instrumented indentation. Part 3: Rheological model and other characteristics," *Chemicke Listy*, vol. 104, pp. s275–s278, 2010.

[20] A. Kazmierczak-Balata, J. Bodzenta, and D. Trefon-Radziejewska, "Determination of Thermal-Diffusivity Dependence on Temperature of Transparent Samples by Thermal Wave Method," *International Journal of Thermophysics*, vol. 31, no. 1, pp. 180–186, Jan. 2010, https://doi.org/10.1007/s10765-009-0676-1.

[21] D. Singh, "Passenger body vibration control in active quarter car model using ANFIS based super twisting sliding mode controller," *Simulation Modelling Practice and Theory*, vol. 89, pp. 100–118, Dec. 2018, https://doi.org/10.1016/j.simpat.2018.09.010.

[22] E. Yildirim and I. Esen, "Dynamic Behavior and Force Analysis of the Full Vehicle Model using Newmark Average Acceleration Method," *Engineering, Technology & Applied Science Research*, vol. 10, no. 1, pp. 5330–5339, Feb. 2020, https://doi.org/10.48084/etasr.3335.

[23] I. Celinski, R. Burdzik, J. Mlynczak, and M. Klaczynski, "Research on the Applicability of Vibration Signals for Real-Time Train and Track Condition Monitoring," *Sensors*, vol. 22, no. 6, Jan. 2022, Art. no. 2368, https://doi.org/10.3390/s22062368.

[24] R. Burdzik, "Impact and Assessment of Suspension Stiffness on Vibration Propagation into Vehicle," *Sensors*, vol. 23, no. 4, Jan. 2023, Art. no. 1930, https://doi.org/10.3390/s23041930.

[25] M. Issa and A. Samn, "Passive vehicle suspension system optimization using Harris Hawk Optimization algorithm," *Mathematics and Computers in Simulation*, vol. 191, pp. 328–345, Jan. 2022, https://doi.org/10.1016/j.matcom.2021.08.016.

[26] A. C. Mitra, G. J. Desai, S. R. Patwardhan, P. H. Shirke, W. M. H. Kurne, and N. Banerjee, "Optimization of Passive Vehicle Suspension System by Genetic Algorithm," *Procedia Engineering*, vol. 144, pp. 1158–1166, Jan. 2016, https://doi.org/10.1016/j.proeng.2016.05.087.

[27] N. Wu, C. Liu, Z. Yang, and Z. Lian, "Structural Design of Special Vehicle Components Based on Topology Optimization," *International Journal of Automotive Technology*, vol. 24, no. 2, pp. 541–549, Apr. 2023, https://doi.org/10.1007/s12239-023-0045-2.

[28] R. Desai, A. Guha, and P. Seshu, "Modelling and simulation of an integrated human-vehicle system with non-linear cushion contact force," *Simulation Modelling Practice and Theory*, vol. 106, Jan. 2021, Art. no. 102206, https://doi.org/10.1016/j.simpat.2020.102206.

[29] S. Latreche and S. Benaggoune, "Robust Wheel Slip for Vehicle Anti-lock Braking System with Fuzzy Sliding Mode Controller (FSMC)," *Engineering, Technology & Applied Science Research*, vol. 10, no. 5, pp. 6368–6373, Oct. 2020, https://doi.org/10.48084/etasr.3830.

[30] H. von Chappuis, G. Mavros, P. King, and H. Rahnejat, "Prediction of impulsive vehicle tyre-suspension response to abusive drive-over-kerb manoeuvres," *Proceedings of the Institution of Mechanical Engineers, Part K: Journal of Multi-body Dynamics*, vol. 227, no. 2, pp. 133–149, Jun. 2013, https://doi.org/10.1177/1464419312469756.

[31] W. Abbas, O. B. Abouelatta, M. El-Azab, M. El-Saidy, and A. A. Megahed, "Optimal Seat Suspension Design Using Genetic Algorithms," *Journal of Mechanics Engineering and Automation*, vol. 1, pp. 44–52, 2011.

[32] V. Goga and M. Klucik, "Optimization of Vehicle Suspension Parameters with use of Evolutionary Computation," *Procedia Engineering*, vol. 48, pp. 174–179, Jan. 2012, https://doi.org/10.1016/j.proeng.2012.09.502.

[33] O. Gundogdu, "Optimal seat and suspension design for a quarter car with driver model using genetic algorithms," *International Journal of Industrial Ergonomics*, vol. 37, no. 4, pp. 327–332, Apr. 2007, https://doi.org/10.1016/j.ergon.2006.11.005.

[34] A. Shirahatti, P. S. S. Prasad, P. Panzade, and M. M. Kulkarni, "Optimal design of passenger car suspension for ride and road holding," *Journal of the Brazilian Society of Mechanical Sciences and Engineering*, vol. 30, pp. 66–76, Mar. 2008, https://doi.org/10.1590/S1678-58782008000100010.

[35] M. Mirzaei and R. Hassannejad, "Application of genetic algorithms to optimum design of elasto-damping elements of a half-car model under random road excitations," *Proceedings of the Institution of Mechanical*

Engineers, Part K: Journal of Multi-body Dynamics, vol. 221, no. 4, pp. 515–526, Dec. 2007, https://doi.org/10.1243/14644193JMBD101.

[36] M. Mitschke, *Dynamik der Kraftfahrzeuge*, 3rd edition. New York, NY, USA: Springer, 1995.

[37] B.-S. Chen, *Multi-Objective Optimization System Designs and Their Applications*. Boca Raton, FL, USA: CRC Press, 2023.

[38] C. Chen, J. Twycross, and J. M. Garibaldi, "A new accuracy measure based on bounded relative error for time series forecasting," *PLOS ONE*, vol. 12, no. 3, Mar. 2017, Art. no. e0174202, https://doi.org/10.1371/journal.pone.0174202.